ORIGINAL ARTICLE

Impaired Epidermal Ceramide Synthesis Causes Autosomal Recessive Congenital Ichthyosis and Reveals the Importance of Ceramide Acyl Chain Length

Katja-Martina Eckl[1,2], Rotem Tidhar[3], Holger Thiele[4], Vinzenz Oji[5], Ingrid Hausser[6], Susanne Brodesser[7,8], Marie-Luise Preil[9], Aysel Önal-Akan[1], Friedrich Stock[10], Dietmar Müller[10], Kerstin Becker[1], Ramona Casper[1], Gudrun Nürnberg[4], Janine Altmüller[4], Peter Nürnberg[4,8], Heiko Traupe[5], Anthony H. Futerman[3] and Hans C. Hennies[1,2,8]

The barrier function of the human epidermis is supposed to be governed by lipid composition and organization in the stratum corneum. Disorders of keratinization, namely ichthyoses, are typically associated with disturbed barrier activity. Using autozygosity mapping and exome sequencing, we have identified a homozygous missense mutation in *CERS3* in patients with congenital ichthyosis characterized by collodion membranes at birth, generalized scaling of the skin, and mild erythroderma. We demonstrate that the mutation inactivates ceramide synthase 3 (CerS3), which is synthesized in skin and testis, in an assay of *N*-acylation with C26-CoA, both in patient keratinocytes and using recombinant mutant proteins. Moreover, we show a specific loss of ceramides with very long acyl chains from C26 up to C34 in terminally differentiating patient keratinocytes, which is in line with findings from a recent CerS3-deficient mouse model. Analysis of reconstructed patient skin reveals disturbance of epidermal differentiation with an earlier maturation and an impairment of epidermal barrier function. Our findings demonstrate that synthesis of very long chain ceramides by CerS3 is a crucial early step for the skin barrier formation and link disorders presenting with congenital ichthyosis to defects in sphingolipid metabolism and the epidermal lipid architecture.

Journal of Investigative Dermatology (2013) **133,** 2202–2211; doi:10.1038/jid.2013.153; published online 9 May 2013

INTRODUCTION

The barrier function of the human epidermis is localized to the outermost layer, the stratum corneum. Its main tasks comprise protection of the organism from intrusion of pathogens and other exogenous influences as well as from dehydration through excessive transepidermal water loss. The stratum corneum is composed of compact lamellar structures mounted by cornified envelopes, which derive from terminally differentiated keratinocytes, and a typical pattern of lipids that are secreted into the lamellar interspaces and make up the lipid envelope (Lazo *et al.*, 1995; Marekov and Steinert, 1998). The stratum corneum was thus described as a wall composed of bricks (corneocytes) and mortar (lipids) (Elias, 1987).

The lamellar lipids consist of approximately equal amounts of ceramides, cholesterol, and free fatty acids. Early *in vitro* experiments demonstrated that the permeability and integrity of bilayered structures is crucially influenced by the inclusion of ceramides (Lopez *et al.*, 1999). Studies of the human stratum corneum identified more than 11 different types of ceramides (Masukawa *et al.*, 2008; van Smeden *et al.*, 2011), with very typical structures that are unique or rarely found in other tissues and species: in esterified ω-hydroxy ceramides

[1]*Center for Dermatogenetics, Cologne Center for Genomics, University of Cologne, Cologne, Germany;* [2]*Center for Dermatogenetics, Division of Human Genetics and Department of Dermatology, Innsbruck Medical University, Innsbruck, Austria;* [3]*Department of Biological Chemistry, Weizmann Institute of Science, Rehovot, Israel;* [4]*Cologne Center for Genomics, University of Cologne, Cologne, Germany;* [5]*Department of Dermatology, University Hospital of Münster, Münster, Germany;* [6]*Department of Dermatology, University Hospital of Heidelberg, Heidelberg, Germany;* [7]*Institute of Medical Microbiology, Immunology and Hygiene, University of Cologne, Cologne, Germany;* [8]*Cluster of Excellence on Cellular Stress Responses in Aging-Associated Diseases, University of Cologne, Cologne, Germany;* [9]*Practice for Dermatology Dres. Krnjaic, Merk, Preil, and Schäfer, Ansbach, Germany and* [10]*Institute of Human Genetics, University Hospital of Leipzig, Leipzig, Germany*

Correspondence: Hans C. Hennies, Center for Dermatogenetics, Division of Human Genetics, Innsbruck Medical University, 6020 Innsbruck, Austria. E-mail: h.hennies@i-med.ac.at

Abbreviations: ARCI, autosomal recessive congenital ichthyosis; CerS3, ceramide synthase 3; EOS, esterified ω-hydroxyacyl sphingosine; HEK, human embryonic kidney; LC-ESI-MS/MS, liquid chromatography coupled to electrospray ionization tandem mass; LOX, lipoxygenase; OMIM, Online Mendelian Inheritance in Man

Received 24 September 2012; revised 25 February 2013; accepted 27 February 2013; accepted article preview online 2 April 2013; published online 9 May 2013

with a sphingosine, phytosphingosine, or hydroxysphingosine base, linoleic acid is ester-linked to a very long acyl chain ceramide with ⩾C30. Recent *in vitro* data have pointed out the importance of long hydrophobic chains of ceramides to maintain the skin barrier function (Janušová *et al.*, 2011), and an analysis of the lipid matrix *in situ* has shown that the human skin barrier is organized by stacked bilayers of fully extended ceramides and cholesterol molecules associated with the sphingoid base (Iwai *et al.*, 2012).

The activity of the epidermal permeability barrier is typically compromised in several keratinization disorders, in particular ichthyoses, disorders affecting all or most of the skin with scaling, hyperkeratosis, and/or erythroderma (Bouwstra and Ponec, 2006; Schmuth *et al.*, 2007; Elias *et al.*, 2008). Autosomal recessive congenital ichthyosis (ARCI) is a heterogeneous group of rare, severe disorders with an approximate prevalence of 1:100,000 (Oji *et al.*, 2010). Mutations associated with ichthyosis were described in more than 40 genes until today. Several phenotypes presenting with ichthyosis, however, cannot be attributed to mutations in one of these genes. Moreover, the pathogenic context of these disorders remains elusive in many cases. Here we have identified mutations in *CERS3*, the gene encoding ceramide synthase 3, as a cause of ARCI. The impairment of enzyme activity leads to a disturbed epidermal permeability barrier function and indicates the important role of ceramides with very long acyl chains in differentiating keratinocytes.

RESULTS

Identification of mutations in *CERS3*

We have identified a large family with congenital ichthyosis from Germany with multiple consanguinity (Figure 1). The

Figure 1. Phenotype and pedigree. (**a**) Clinical characterization of patient VII:3 at the age of (i) 6 days, (ii and iii) 3 years, and (iv) 7 years. The girl was born as collodion baby and developed a moderate lamellar ichthyosis with pronounced keratotic lichenification with a prematurely aged appearance. (v) Hematoxylin and eosin (H&E) staining of skin sections demonstrated compact orthohyperkeratosis with mild acanthosis. (**b**) The pedigree contains multiple consanguinity. Question marks denote connections where the exact relationship is unknown. Individuals marked with a bar were clinically investigated by one of us. Subjects marked with + or # sign were included in the linkage analysis and samples from VI:4, VI:13, and VII:1 in the exome sequencing.

pedigree comprised several branches with a total of nine individuals diagnosed with ARCI, five of whom seen by us. The girl VII:3 was investigated in detail over her lifetime (Figure 1a). At birth, she presented an extreme ectropion and eclabium with collodion membranes, which rapidly resolved within 1 week. Since then, she showed a moderate lamellar ichthyosis with mild erythroderma, with an improvement in the summer period. In addition, she reported hypohidrosis, but sweating was possible on the back of her nose. At the age of 3 years, she showed severe scaling of the scalp and a pronounced keratotic lichenification with a prematurely aged appearance. She suffered from repeated uncomplicated bacterial and pityrosporum infections of the skin on her back and from pruritus. At 7 years of age, the scaling was lighter in color and milder and she exhibited exacerbated erythroderma. Strong keratotic lichenification was still present. History of atopic diseases was negative. Light microscopy revealed a moderate and compact orthohyperkeratosis with hyperplastic, papillomatous epidermis, and mild acanthosis (Figure 1a). It is noteworthy that the patient was never treated with systemic retinoids but was advised to take a daily bath with small amounts of $NaHCO_3$ as a bath additive to carry out mechanical scale removal with the help of a glove while still in the bath, and to apply supportive emollients containing, e.g., 5% dexpanthenol and up to 2% urea to the skin afterward. This treatment strategy, which is in line with the recommendations from the literature (Oji and Traupe, 2009), is aimed at ameliorating the phenotype and not known to alter the type of the disease within the spectrum of clinical presentations of congenital ichthyosis.

We received written informed consent from all individuals enrolled. The study was approved by the institutional ethics committee and followed the Declaration of Helsinki Principles. We extracted DNA from peripheral blood samples of 19 probands and analyzed known genes for ARCI without a finding. We then used samples from 15 family members (Figure 1b) for linkage analysis using the Affymetrix GeneChip Human Mapping 250K Sty Array Set. Genome-wide analysis with 20,000 markers assuming three separate consanguineous families gave only one significant finding, with a LOD score of 4.2, which increased to 6.9 in a refined analysis of the interval using all markers from the array set. The overlapping homozygous interval between rs12101356 and the most telomeric marker on chromosome 15q, rs11637017, was 3.4 Mb in length and contained 54 genes and transcripts.

In parallel, we performed whole exome sequence analysis using samples from three family members, two affected and one obligatory heterozygote (see Supplementary Materials and Methods online). The mean sequence coverage was 90x, 88% of target sequences were covered at least 10-fold, and 76% at least 30-fold. After filtering against public databases of known variants in the human genome such as Single Nucleotide Polymorphism Database (dbSNP) or 1,000 Genomes, we found two variants in the interval on 15q26-qter, in ENSG00000223792 and *CERS3*. Only one variant, c.43T>C in exon 4 of *CERS3*, was consistent with autozygosity. Analysis of this variant in the whole family using conventional sequence analysis confirmed full cosegregation of the mutation (Supplementary Figure S1 online), and the mutation was not found on 200 chromosomes from control individuals. Next, we analyzed samples from 80 unrelated individuals diagnosed with ARCI who did not have mutation findings in previously known candidate genes, but we did not identify another mutation in *CERS3* in these samples. The mutation results in a codon exchange p.Trp15Arg in CerS3, also known as *longevity assurance gene-1* (*LAG1*) homolog-3. The residue Trp15 is particularly conserved, both through the family of human LAG1 proteins and in orthologous proteins (Supplementary Figure S2 online), as represented by a conservation score of 9 (highly conserved) in ConSurf (Ashkenazy *et al.*, 2010). The mutation is predicted to be damaging with a SIFT (Sorting Intolerant From Tolerant) score (Ng and Henikoff, 2001) of 0 and a PolyPhen score (Adzhubei *et al.*, 2010) of 0.998.

Gene expression analysis in CerS3-deficient skin

To further characterize the importance of the mutation p.Trp15Arg, we extracted RNA from cultured keratinocytes and quantified *CERS3* transcripts with real-time reverse-transcriptase–PCR. *CERS3* mRNA amounts were mildly reduced to 70% in patient cells. We then analyzed the expression of CerS3 and several key components of terminally differentiating keratinocytes using immunohistochemistry on sections from patients and controls (Supplementary Materials and Methods online). We observed the synthesis of CerS3 in the granular layer of the epidermis and in particular in the transition zone between stratum granulosum and stratum corneum (Figure 2a–c). The specificity of the signal was confirmed by analyzing reconstructed skin deficient for CerS3 (Supplementary Figure S3 online). Signals of CerS3 in sections from patient epidermis were slightly reduced but clearly present in accordance with our results from RNA quantitation. They were broader in patient skin and also visible in the stratum corneum (Figure 2b and c). We also observed a partly upregulated and broadened expression of involucrin, loricrin, and filaggrin in patient skin (Figure 2d). Expression of structural proteins of basal and suprabasal keratinocytes, e.g. keratins, was unchanged (Figure 2e). The expression of 12*R*-lipoxygenase (12*R*-LOX) was clearly upregulated in patient skin and also visible deep in the spinous layer, in contrast to control sections, where it was only present in the upper granular layer (Figure 2f). Relative quantitation of transcripts from *ALOX12B* and *ALOXE3*, the genes for the two epidermal lipoxygenases 12*R*-LOX and eLOX-3, showed that their amounts were strongly increased to 232% and 149%, respectively, in patient keratinocytes compared with terminally differentiated control keratinocytes.

Impairment of very long acyl chain ceramide synthesis

CerS3 specifically synthesizes very long acyl chain ceramides with lengths of $\geqslant$C26. We have therefore analyzed the activity of protein lysates from differentiated control and patient keratinocytes toward C26–acyl–coenzyme A (CoA), demonstrating clearly reduced levels of C26 ceramide synthesis with patient cell homogenates (Figure 2g). Next, we cloned wild-type and mutant (Trp15Arg) *CERS3* and

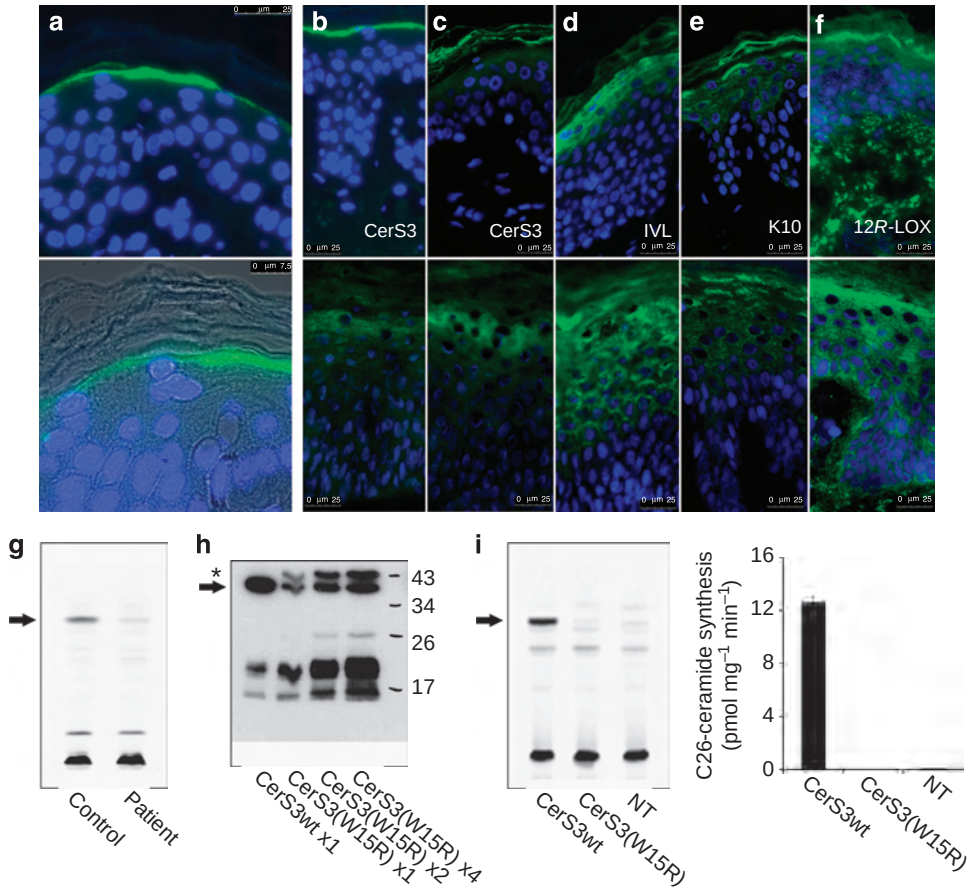

Figure 2. Synthesis and activity of ceramide synthase 3 (CerS3). (**a**) Specific expression of *CERS3* in the uppermost layer of the stratum granulosum and the transit zone to the stratum corneum in healthy skin as shown by immunohistochemistry with and without bright field depiction of the epidermis. (**b**–**f**) CerS3 and markers of epidermal differentiation in healthy (upper part) and patient skin (lower part). (**b**, **c**) Analysis of CerS3 with two different antibodies showed distinctive expression in the upper stratum granulosum in healthy skin in contrast to more diffuse expression in the granular and horny layers in the patient sample. Expression of (**d**) involucrin (IVL) was elevated and broader in patient skin. (**e**) Keratin 10 (K10) was unchanged in patient samples. Detection of (**f**) 12*R*-lipoxygenase (12*R*-LOX) was markedly broadened in the patient sample. Antibodies: green, 4′,6-diamidino-2-phenylindole (DAPI): blue. Scale bars = 25 μm. (**g**–**i**) Ceramide synthase activity. (**g**) Intrinsic CerS3 was assayed using C26–coenzyme A (CoA) in homogenates from primary keratinocytes and lipids were separated by thin layer chromatography. $N = 3$. (**h**) Western blot analysis confirmed expression of recombinant CerS3 in human embryonic kidney (HEK) cells and showed slightly reduced amounts of mutant CerS3 compared with wild type (arrow). The upper band seen here is supposed to represent an alternatively glycosylated form of CerS3 (Laviad *et al.*, 2012; asterisk). (**i**) Overexpression of CerS3 indicated almost complete loss of enzyme activity caused by mutation p.Trp15Arg *in vitro*. NT, transfection control. Means ± SD; $N = 3$.

overexpressed the constructs in human embryonic kidney (HEK) cells. Both wild-type and mutant CerS3 were synthesized in these cells (Figure 2h); however, amounts of mutant enzyme were reduced somewhat compared with wild type. Homogenates of HEK cells expressing wild-type *CERS3* showed *N*-acylation using C26–CoA, which was almost completely lacking in lysates from HEK cells expressing mutant *CERS3* (Figure 2i). In order to determine the effects of CerS3 impairment in our patients, we further analyzed the levels of free (not protein-bound) and protein-bound ceramides in terminally differentiating keratinocytes from the patient compared with keratinocytes isolated from control subjects matched in age, skin type, and origin using liquid chromatography/tandem mass spectrometry (LC-MS/MS). These studies revealed a strong lack of very long chain ceramides in patient keratinocytes (Figure 3), as shown for nonhydroxylated and nonesterified hydroxylated ceramides, ω-hydroxylated ceramides esterified with linoleate (EOS), as well as protein-bound ω-hydroxylated ceramides. The decrease was most obvious for nonhydroxylated and hydroxylated ceramides with C26:0 and longer fatty acyl chains ($P<10^{-4}$ for C30:0), for ⩾C30:0 chain EOS ceramides ($P<10^{-2}$ for C34:0), and for ⩾C30:0 chain protein-bound hydroxylated ceramides ($P<10^{-5}$).

Disturbed epidermal differentiation and impaired epidermal barrier function

To study the consequences of lack of long chain ceramides, we further analyzed the morphology of patient skin. Ultrastructural analysis of skin biopsy specimens of patients VII:1 and VII:3 showed mild acanthosis and moderate to strong orthohyperkeratosis with cleft-like inclusions in the stratum corneum, possibly originating from unaccomplished vesicular trafficking due to not properly processed neutral lipids and

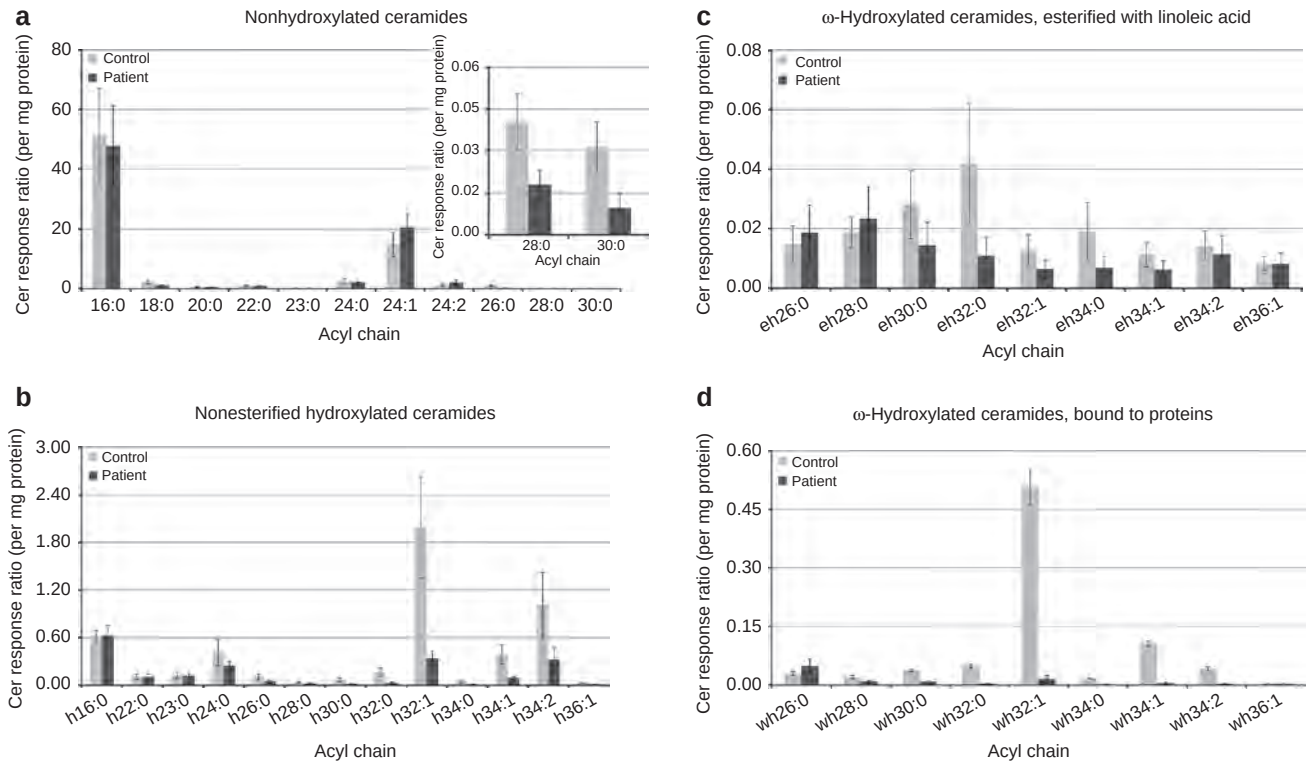

Figure 3. Loss of very long acyl chain ceramides in patient keratinocytes. Free and protein-bound ceramides extracted from differentiated keratinocytes from patient and healthy controls were analyzed with liquid chromatography coupled to electrospray ionization tandem mass spectrometry (LC-ESI-MS/MS). (**a**) Free nonhydroxylated ceramides, (**b**) free nonesterified hydroxylated ceramides, (**c**) free ω-hydroxylated ceramides esterified with linoleic acid, and (**d**) protein-bound ω-hydroxylated ceramides. Cer response ratio refers to the integrated peak area of the defined endogenous ceramide divided by the peak area of the internal standard. Means ± SD; $N = 2$ analytical replicates of $N = 4$ biological replicates.

partly containing melanosomal remnants, and irregular vesicular structures in the granular layer (Figure 4a). Unfortunately, the quality of the fixed material obtained was insufficient for more detailed studies and the family did not consent to provide fresh skin specimens. However, here we did not find a clear clue to a premature lamellar body front in lower granular layers as there were no morphological hallmarks for keratinocyte maturation arrest, which is in contrast to the findings reported in CerS3-deficient mice (Jennemann *et al.*, 2012).

We then used organotypic cell cultures to model the patient skin. We cultured keratinocytes and fibroblasts isolated from a punch biopsy of patient VII:3 and established three-dimensional full-thickness skin models consisting of a dermal matrix with fibroblasts and an epidermal compartment of keratinocytes. Disease models represented the morphological features of patient skin (Supplementary Figure S4 online). The analysis clearly illustrated the presence of CerS3 in the upper granular layer and the stratum corneum in control and patient models, where the expression was broader and extended to earlier epidermal layers (Figure 4c). Characterization of skin models with markers of basal and suprabasal epidermal architecture did not show clear changes. Analysis of markers for keratinocyte terminal differentiation demonstrated earlier maturation and partly stronger expression (Figure 4d and e). Electron microscopy of patient skin models demonstrated a thickened, compact stratum corneum with inhomogeneous lamellae and regular-appearing cornified cell envelopes and showed reduced quantities of keratohyalin and only single lamellar bodies in upper suprabasal layers. Fusion of lamellar bodies in the transition zone was not obvious and multiple lipid droplets and other vesicular inclusions were visible in the stratum corneum (Figure 4b). Taken together, these findings point to an immature cornification process. To analyze the epidermal barrier function, we used a penetration assay with the water-soluble fluorescent dye Lucifer Yellow on reconstructed skin. The assays revealed reduced permeability barrier activity in patient models compared with control models (Figure 4f and g). Barrier impairment, however, was noticeably milder than in ichthyosis skin models deficient for transglutaminase-1 or 12*R*-LOX (Eckl *et al.*, 2011).

DISCUSSION

We have identified a homozygous mutation in *CERS3* as a cause for congenital ichthyosis using a combined strategy of autozygosity mapping and exome sequencing. Ceramide synthases contain two common motifs, a homeobox (Hox) domain (residues 83–127 in CerS3) and a TRAM, LAG1, and CLN8 (TLC) domain (residues 130–331). Directed experiments in members of the ceramide synthase protein family suggested the active site in the Lag1p motif, which is part of the TLC domain (Kageyama-Yahara and Riezman,

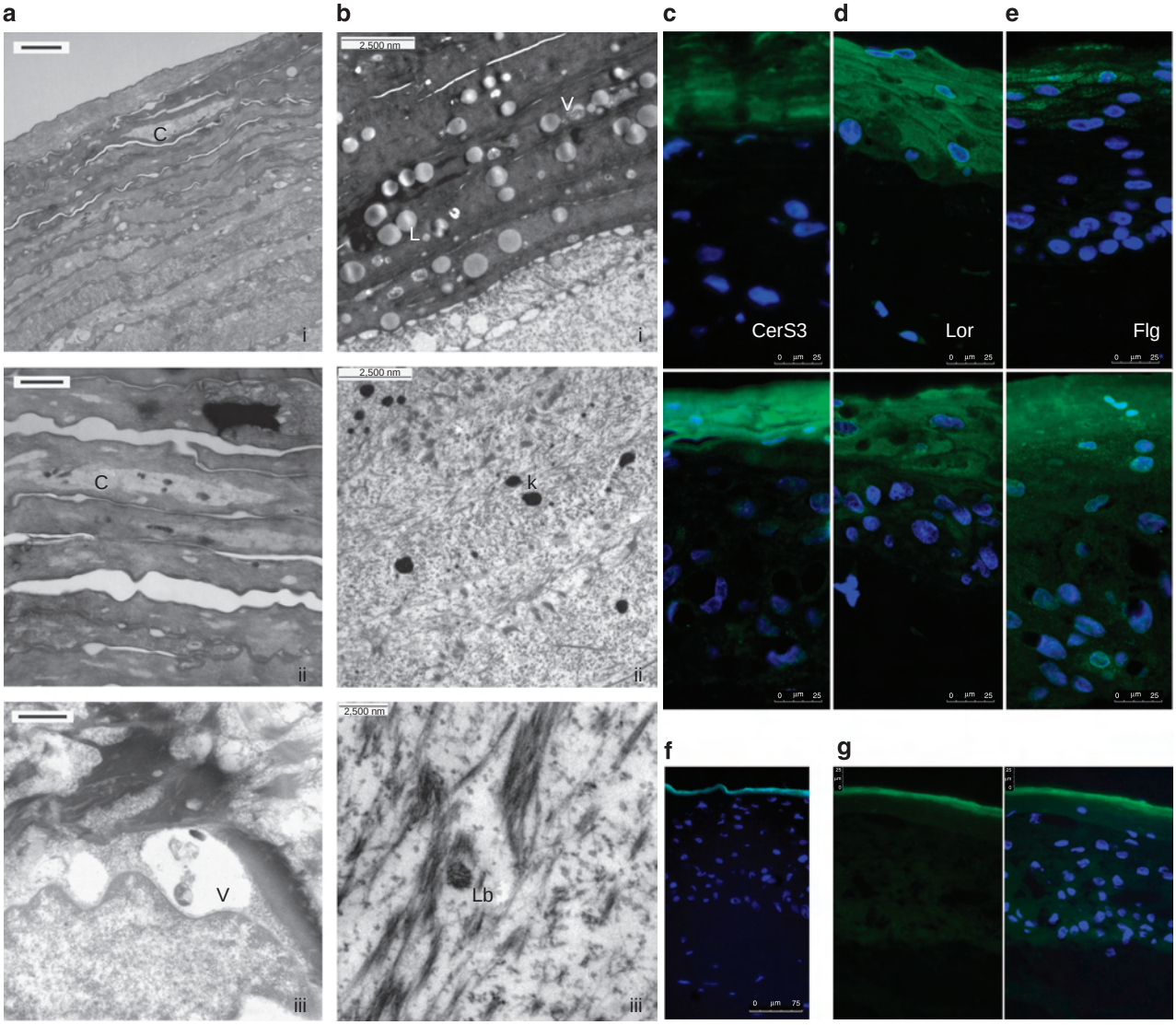

Figure 4. Morphological characterization of patient skin and disease models. (**a**) Ultrastructural analysis of skin biopsy specimens of patients VII:1 and VII:3 showed mild acanthosis and moderate to strong orthohyperkeratosis. Cleft-like inclusions (C), possibly originating from unprocessed neutral lipids and partly containing melanosomal remnants, were frequently visible in horny lamellae, and irregular vesicular structures (V), partly with melanosomes, were present in the granular layer. Scale bars = 2 µm (i), 1 µm (ii), 500 nm (iii). (**b**) Reconstructed skin of patient VII:3 showed a compact, thickened stratum corneum with inhomogeneous lamellae and inconspicuous cornified cell envelopes. Lipid droplets (L) and vesicular inclusions (V) were frequently visible in the stratum corneum. Numbers of keratohyalin granules (k) and lamellar bodies (Lbs) were reduced and irregularly distributed in suprabasal layers. Scale bars = 2.5 µm (i and ii), 250 nm (iii). (**c**–**e**) Reconstructed skin was characterized by antibodies against markers of epidermal differentiation. (**c**) Ceramide synthase 3 (CerS3) is present in upper granular and horny layers in normal models (upper part) and extended to earlier layers in disease models (lower part). (**d**) Loricrin (Lor) and (**e**) filaggrin (Flg) were present in layers of differentiated keratinocytes in controls (upper part) and also visible in earlier layers in disease models (lower part). Scale bar = 25 µm. (**f**, **g**) Reconstructed skin was used for dye penetration assays with Lucifer Yellow. Compared with (**f**) healthy skin, the permeability barrier function is reduced in (**g**) disease models as shown by visualization of Lucifer Yellow (left) and overlay with 4′,6-diamidino-2-phenylindole (DAPI) staining (right). Scale bars = 75 µm (**f**), 25 µm (**g**).

2006; Spassieva *et al.*, 2006). A functional motif adjacent to Hox and TLC domains is essential for enzyme activity; on the other hand, a major part of the Hox domain appears to be dispensable (Mesika *et al.*, 2007). A motif of ~30 residues in the N-terminal domain of CerS3 and particularly the tryptophan residue at position 15 are extremely conserved, pointing to the importance of the domain for protein function.

CerS3 belongs to the protein family of ceramide synthases based on their homology with yeast LAG1p (Mizutani *et al.*, 2006; Rabionet *et al.*, 2008). Ceramide synthases form dihydroceramide from sphinganine by *N*-acylation of the sphingoid base (Pewzner-Jung *et al.*, 2006; Teufel *et al.*, 2009; Levy and Futerman, 2010; Mullen *et al.*, 2012), and six human ceramide synthases can be differentiated by their tissue specificity and the specificity for certain acyl–CoA chain

lengths. *CERS3* is mainly expressed in testis and the skin; and CerS3 and CerS4 are the major ceramide synthases of the skin (Laviad *et al.*, 2008). CerS3 is exceptional as it is able to metabolize an extended spectrum of very long acyl chains (Mizutani *et al.*, 2008). Epidermal keratinocytes are unique with regard to the presence of certain ceramide species and the importance of very long chain fatty acids. We detected the major defect in patient cells toward ceramides with acyl chain lengths $\geqslant$C26 and up to C36. We found the loss of very long chain ceramides in various ceramide species and both in free and protein-bound ceramides. Our findings are in line with the assumption that EOS ceramides are generated from free hydroxylated ceramides in the epidermis and are essential for the binding of ceramides to cornified envelope proteins (Doering *et al.*, 1999; Nemes *et al.*, 1999; Uchida and Holleran, 2008). Human CerS3 is mainly expressed in the transition zone between granular layer and stratum corneum, and we found the specific failure in ceramide synthesis only in terminally differentiated patient keratinocytes (data not shown). We detected reduced levels of mutant CerS3 synthesis *in vitro*; however, the protein is clearly present and the reduction in protein levels alone probably cannot explain the loss of activity. Thus, we suggest that the deficit of very long chain ceramides is mainly due to a vast inactivation of CerS3. Residual activity of mutant CerS3 *in vivo* could be involved in the observed synthesis of small amounts of very long chain ceramides in patient cells. Moreover, some limited compensation for missing CerS3 activity might take place through other members of the human ceramide synthase family such as CerS2, which can synthesize C22–C26 ceramides, the latter although to a limited extent.

The broadened expression of key components of terminal keratinocyte differentiation, in contrast to normal expression of structural proteins of basal and suprabasal keratinocytes, indicates a disturbed epidermal differentiation and a premature keratinization resulting from the loss of CerS3 activity. This finding is consistent with data obtained from a recent *Cers3* knockout mouse line (Jennemann *et al.*, 2012), which demonstrated a severe skin barrier defect leading to death of mutant mice shortly after birth accompanied by a deficiency in epidermal keratinization and a strong increase in transepidermal water loss. It is still not clear in detail why the human disease is compatible with life; however, the discrepancy may reflect the different stages of skin development in mice and humans at birth. The ratio of body volume to surface is beneficial in humans compared with rodents to reduce dehydration; moreover, the intrauterine development of a collodion membrane in affected humans diminishes the immediate neonatal transepidermal water loss that is present in the mouse models of ARCI studied so far. Our results are also corroborated by the finding of a thick, compact stratum corneum with lipid enclosures, reduced amounts of lamellar bodies and keratohyalin, and irregularly processed vesicular structures in patient skin and CerS3-deficient skin models.

From a pathophysiologic point of view, different types of congenital ichthyosis have abnormalities in the epidermal permeability barrier in common (Bouwstra and Ponec, 2006; Schmuth *et al.*, 2007; Elias *et al.*, 2008; Oji *et al.*, 2010). These diseases comprise, among others, forms of ARCI including Harlequin ichthyosis (Online Mendelian Inheritance in Man (OMIM) 242500), a particularly severe form of nonsyndromic congenital ichthyosis caused by mutations in *ABCA12*, lamellar ichthyosis, and congenital ichthyosiform erythroderma, which can be caused by mutations in transglutaminase-1, 12*R*-LOX, eLOX-3, and others (OMIM 242100, 242300). Notably, the elongation of very long chain fatty acids involves *ELOVL4*, which can be mutated in a syndrome of ichthyosis, intellectual disability, and spastic quadriplegia (OMIM 614457) (Aldahmesh *et al.*, 2011). Similarly, *FATP4*, which is mutated in ichthyosis prematurity syndrome (OMIM 608649) (Klar *et al.*, 2009), can serve as a very long chain acyl–CoA synthetase (Jia *et al.*, 2007), which might be essential in late fetal development but substituted soon after birth. Very long chain acyl–CoA and sphinganine are then substrates of CerS3 to form (dihydro)ceramides, which are transported from the endoplasmic reticulum to the Golgi apparatus, glycosylated, and further transferred to lamellar bodies. These contain membrane-bound transporter proteins including ABCA12, which might be involved in transport of glucosylceramides and fatty acids (Akiyama *et al.*, 2005), and glucosylceramides are then esterified with linoleate (Hamanaka *et al.*, 2002), which is provided by hydrolysis of triacylglycerol (Uchida *et al.*, 2010). Mutations in *ABHD5* (encoding CGI-58) can cause neutral lipid storage disease with ichthyosis (Chanarin–Dorfman syndrome; OMIM 275630). CGI-58 has been identified as a cofactor for triacylglyceride lipase and acts as an acyl transferase (Montero-Moran *et al.*, 2010; Radner *et al.*, 2010). Accordingly, loss of CGI-58 leads to a decrease in EOS ceramides and bound ω-hydroxylated ceramides but an increase in free ω-hydroxylated ceramides (Radner *et al.*, 2010; Uchida *et al.*, 2010). Recent data have shown that EOS ceramides are finally oxygenated in a two-step process by 12*R*-LOX and eLOX-3 (Zheng *et al.*, 2011). Oxidized linoleate is hydrolyzed and glucosylceramide deglycosylated by β-glucocerebrosidase, which can be mutated in Gaucher disease (OMIM 230900) (Holleran *et al.*, 1994). Extended ceramides are then covalently linked to the cornified envelope by transglutaminase-1 (Nemes *et al.*, 1999) and thus available for the barrier formation as stacked bilayers (Iwai *et al.*, 2012).

To conclude, our results significantly contribute to the emerging evidence for the understanding that congenital ichthyosis is a disorder of disturbed lipid metabolism in the skin, regardless of the underlying genetic cause (Elias *et al.*, 2012). They pinpoint the specific importance of very long chain ceramides for the epidermal differentiation and barrier integrity and the formation of the cornified lipid envelope (Behne *et al.*, 2000; Uchida and Holleran, 2008). Several diseases presenting with ichthyosis and barrier disturbance can thus be attributed to defects of ceramide synthesis and delivery. Further experiments are necessary to characterize the interconnection of the proteins involved in more detail; however, an avenue is laid open to targeted therapeutic strategies, as a common pathological context is apparent and disease-specific interventions are yet possible.

MATERIALS AND METHODS

Linkage and exome sequence analysis

Peripheral blood was collected in EDTA from all available family members and DNA was extracted using standard procedures. DNA samples were genotyped using the Affymetrix GeneChip Human Mapping 250K Sty Array Set. Genotypes were called by the GeneChip DNA Analysis Software (Affymetrix, Santa Clara, CA) and all data were handled using the graphical user interface ALOHOMORA (Rüschendorf and Nürnberg, 2005). Data were checked using the program Graphical Representation of Relationships (Abecasis *et al.*, 2001), and parametric linkage analysis was done with the programs Allegro (Gudbjartsson *et al.*, 2005) and MERLIN (Abecasis *et al.*, 2002). Exome sequencing was done after enrichment with the Agilent SureSelect Human All Exome 50 Mb kit (Agilent, Santa Clara, CA) using the Illumina GAIIx sequencing instrument (Illumina, San Diego, CA) with a single end read 150 bp protocol (see Supplementary Materials and Methods online).

Reverse-transcriptase–PCR

RNA was extracted from cultured keratinocytes using the RNeasy Mini Kit (Qiagen, Hilden, Germany). Relative quantification was performed with a one-step reverse-transcriptase–PCR protocol using the SYBR GreenER Kit (Life Technologies, Darmstadt, Germany) and analyzed in a LightCycler 480 Real-Time PCR System (Roche Diagnostics, Mannheim, Germany) with reference to 18S RNA, *GAPDH*, and *RPS18*. Primers used were as follows: *CERS3* forward (F): 5′-CCAGGCTGAAGAAATTCCAG-3′, and reverse (R): 5′-AACGC AATTCCAGCAACAGT-3′; *ALOX12B* F: 5′-ACCCGAGGGCAAGA TGAT-3′, and R: 5′-GCAGGAAGATGGGGCAAT-3′; *ALOXE3* F: 5′-AAGCTTCGAGGGCTGTTG-3′, and R: 5′-CACCAGTGCTCTGTG ACATACTT-3′.

Electron microscopy

Specimens were fixed at room temperature in 3% glutaraldehyde in 0.1 M cacodylate buffer, pH 7.4, cut into pieces of 1 mm^3, washed in buffer, postfixed for 1 hour at 4 °C in 1% osmium tetroxide, rinsed in water, dehydrated through graded ethanol solutions, transferred into propylene oxide, and embedded in epoxy resin (Glycidether 100, Carl Roth, Karlsruhe, Germany). Semithin and ultrathin sections were cut with an ultramicrotome (Ultracut E, Reichert, Göttingen, Germany). Ultrathin sections were treated with uranyl acetate and lead citrate, and examined with an electron microscope (EM 900, Zeiss, Oberkochen, Germany).

Cell culture

Biopsy specimens were used for the isolation of normal human epidermal keratinocytes and normal human dermal fibroblasts as described previously (Eckl *et al.*, 2011). Normal human epidermal keratinocytes were cultured for the first two passages on mitomycin C–treated 3T3 J2 feeders in keratinocyte culture medium (Allen-Hoffmann and Rheinwald, 1984); afterwards, normal human epidermal keratinocytes were grown in the absence of feeder cells under low Ca^{2+} conditions in keratinocyte grown medium (Lonza, Verviers, Belgium) up to passage 4. Differentiated keratinocytes for lipid analysis were obtained in keratinocyte grown medium supplemented with 1.15 mM $CaCl_2$ for 7 days. Normal human dermal fibroblasts were maintained in 10% DMEM. HEK 293T cells were cultured in DMEM supplemented with 10% fetal calf serum, 100 IU ml^{-1} penicillin, and 100 µg ml^{-1} streptomycin. HEK 293T cells were transfected using PEI reagent (Sigma, Munich, Germany).

Transient knockdown of CERS3 in keratinocytes

Knockdown of *CERS3* in basal normal human epidermal keratinocytes was performed with 2,220 pmol of a set of three small interfering RNAs (Life Technologies) and 150 µl Lipofectamin 2000 (Life Technologies) for each T225 flask. The mixture was diluted in Opti-MEM (Life Technologies), and cells remained in serum-free keratinocyte grown medium (Lonza) without any antibiotics. Cells were harvested exactly 24 hours after knockdown and then used for skin model preparation.

Three-dimensional full-thickness skin model preparation

Skin models were prepared as described previously (Eckl *et al.*, 2011) with 3.5–5.2 × 10^6 keratinocytes and 0.25 × 10^6 fibroblasts not older than passages 3 and 4, respectively. Models were cultured in the differentiation medium keratinocyte culture medium (Rheinwald and Green, 1974) at the air–liquid interface for 8 days. Samples were embedded in paraffin or snap frozen. Healthy controls were matched in age, skin type, and origin. For penetration assays, a sterile silicone ring with a 0.8 cm inner diameter was applied and a 1 mM Lucifer Yellow solution was poured onto the skin model. After incubation for 1 hour, models were washed excessively and samples taken using a skin biopsy punch. Cryosections were counterstained with 4′,6-diamidino-2-phenylindole and analyzed with a fluorescence microscope (LMD 6000, Leica, Wetzlar, Germany).

Cloning of CERS3

Total RNA was extracted from differentiated keratinocytes. cDNA synthesis was performed with oligo (dT) primers. The complete coding sequence was amplified using Phusion DNA polymerase (New England Biolabs, Frankfurt, Germany) and cloned using the Gateway technology (Life Technologies). The CerS3(W15R) construct was subcloned from wild-type *CERS3* using restriction-free cloning (van den Ent and Löwe, 2006). Primers used were F: 5′-GGAAA GATTCCGGCTTCCTCCAAC-3′ and R: 5′-GTTGGAGGAAGCCGGA ATCTTTCC-3′.

Ceramide synthase assays

Primary human keratinocytes and transfected HEK cells were homogenized in 20 mM HEPES-KOH, pH 7.2, 25 mM KCl, 250 mM sucrose, and 2 mM $MgCl_2$ containing a protease inhibitor cocktail (Sigma). Protein content was determined using the Bradford reagent (Bio-Rad, Hercules, CA). Homogenates were incubated with 15 µM NBD-sphinganine (Avanti Polar Lipids, Alabaster, AL), 20 µM defatted BSA (Sigma), and 50 µM C26–CoA (Avanti Polar Lipids) for 20 minutes at 37 °C. Lipids were extracted and separated by thin layer chromatography using chloroform, methanol, and 2 M NH_4OH (40:10:1, v/v/v) as the developing solvent. NBD-labeled lipids were visualized using the Typhoon 9410 variable mode imager and quantified by ImageQuantTL (GE Healthcare, Chalfont St Giles, UK).

LC-ESI-MS/MS analysis of ceramides

Ceramides in differentiated keratinocytes were determined by LC coupled to electrospray ionization tandem mass spectrometry (LC-ESI-MS/MS). Cells were homogenized in water (~5 × 10^6 cells per ml) using the Precellys 24 Homogenisator (Peqlab, Erlangen, Germany).

The protein content of the homogenate was determined using bicinchoninic acid. For the analysis of free (not protein-bound) ceramides, 100 µl of homogenate was spiked with 750 µl of methanol/chloroform 2:1 (v/v) and 200 pmol of the internal standard ceramide 17:0 (Matreya, Pleasant Gap, PA). Lipids were extracted overnight at 48 °C. For the analysis of ceramides bound to proteins of the cornified envelope, 1.4 ml of homogenate was used, and ceramides were released as described previously (Jennemann *et al.*, 2012). Lipid extracts were purified using a modification of the Bligh-Dyer procedure (Signorelli and Hannun, 2002). Ceramide species were analyzed using a previously described LC-ESI-MS/MS method (Schwamb *et al.*, 2012) and monitored in the positive ion mode with their specific multiple reaction monitoring transitions (Shaner *et al.*, 2009; Jennemann *et al.*, 2012). Integrated peak areas of endogenous ceramide species were corrected against the peak area of the internal standard ceramide 17:0 and then normalized to the protein content.

CONFLICT OF INTEREST

The authors state no conflict of interest.

ACKNOWLEDGMENTS

We are grateful to the patients and their families for their contribution. This research was supported by grants from the German Federal Ministry for Education and Research as part of the Networks for Rare Diseases (01GM0902) and the ERA-Net for Research Programmes on Rare Diseases (E-Rare-2; 01GM1201), the Deutsche Forschungsgemeinschaft (HE3119/5-1), and Köln Fortune, the research support program of the Medical Faculty of the University of Cologne. AHF is the Joseph Meyerhoff Professor of Biochemistry at the Weizmann Institute of Science.

SUPPLEMENTARY MATERIAL

Supplementary material is linked to the online version of the paper at http://www.nature.com/jid

REFERENCES

Abecasis GR, Cherny SS, Cookson WO *et al.* (2001) GRR: graphical representation of relationship errors. *Bioinformatics* 17:742–3

Abecasis GR, Cherny SS, Cookson WO *et al.* (2002) Merlin - rapid analysis of dense genetic maps using sparse gene flow trees. *Nat Genet* 30:97–101

Adzhubei IA, Schmidt S, Peshkin L *et al.* (2010) A method and server for predicting damaging missense mutations. *Nat Methods* 7:248–9

Akiyama M, Sugiyama-Nakagiri Y, Sakai K *et al.* (2005) Mutations in lipid transporter ABCA12 in harlequin ichthyosis and functional recovery by corrective gene transfer. *J Clin Invest* 115:1777–84

Aldahmesh MA, Mohamed JY, Alkuraya HS *et al.* (2011) Recessive mutations in ELOVL4 cause ichthyosis, intellectual disability, and spastic quadriplegia. *Am J Hum Genet* 89:745–50

Allen-Hoffmann BL, Rheinwald JG (1984) Polycyclic aromatic hydrocarbon mutagenesis of human epidermal keratinocytes in culture. *Proc Natl Acad Sci USA* 81:7802–6

Ashkenazy H, Erez E, Martz E *et al.* (2010) ConSurf 2010: calculating evolutionary conservation in sequence and structure of proteins and nucleic acids. *Nucleic Acids Res* 38:W529–33

Behne M, Uchida Y, Seki T *et al.* (2000) Omega-hydroxyceramides are required for corneocyte lipid envelope (CLE) formation and normal epidermal permeability barrier function. *J Invest Dermatol* 114:185–92

Bouwstra JA, Ponec M (2006) The skin barrier in healthy and diseased state. *Biochim Biophys Acta* 1758:2080–95

Doering T, Proia RL, Sandhoff K (1999) Accumulation of protein-bound epidermal glucosylceramides in beta-glucocerebrosidase deficient type 2 Gaucher mice. *FEBS Lett* 447:167–70

Eckl KM, Alef T, Torres S *et al.* (2011) Full-thickness human skin models for congenital ichthyosis and related keratinization disorders. *J Invest Dermatol* 131:1938–42

Elias PM (1987) Plastic wrap revisited. The stratum corneum two-compartment model and its clinical implications. *Arch Dermatol* 123:1405–6

Elias PM, Williams ML, Feingold KR (2012) Abnormal barrier function in the pathogenesis of ichthyosis: therapeutic implications for lipid metabolic disorders. *Clin Dermatol* 30:311–22

Elias PM, Williams ML, Holleran WM *et al.* (2008) Pathogenesis of permeability barrier abnormalities in the ichthyoses: inherited disorders of lipid metabolism. *J Lipid Res* 49:697–714

Gudbjartsson DF, Thorvaldsson T, Kong A *et al.* (2005) Allegro version 2. *Nat Genet* 37:1015–6

Hamanaka S, Hara M, Nishio H *et al.* (2002) Human epidermal glucosylceramides are major precursors of stratum corneum ceramides. *J Invest Dermatol* 119:416–23

Holleran WM, Ginns EI, Menon GK *et al.* (1994) Consequences of beta-glucocerebrosidase deficiency in epidermis. Ultrastructure and permeability barrier alterations in Gaucher disease. *J Clin Invest* 93:1756–64

Iwai I, Han H, Hollander LD *et al.* (2012) The human skin barrier is organized as stacked bilayers of fully extended ceramides with cholesterol molecules associated with the ceramide sphingoid moiety. *J Invest Dermatol* 132:2215–25

Janušová B, Zbytovska J, Lorenc P *et al.* (2011) Effect of ceramide acyl chain length on skin permeability and thermotropic phase behavior of model stratum corneum lipid membranes. *Biochim Biophys Acta* 1811:129–37

Jennemann R, Rabionet M, Gorgas K *et al.* (2012) Loss of ceramide synthase 3 causes lethal skin barrier disruption. *Hum Mol Genet* 21:586–608

Jia Z, Moulson CL, Pei Z *et al.* (2007) Fatty acid transport protein 4 is the principal very long chain fatty acyl-CoA synthetase in skin fibroblasts. *J Biol Chem* 282:20573–83

Kageyama-Yahara N, Riezman H (2006) Transmembrane topology of ceramide synthase in yeast. *Biochem J* 398:585–93

Klar J, Schweiger M, Zimmerman R *et al.* (2009) Mutations in the fatty acid transport protein 4 gene cause the ichthyosis prematurity syndrome. *Am J Hum Genet* 85:248–53

Laviad EL, Albee L, Pankova-Kholmyansky I *et al.* (2008) Characterization of ceramide synthase 2: tissue distribution, substrate specificity, and inhibition by sphingosine 1-phosphate. *J Biol Chem* 283:5677–84

Laviad EL, Kelly S, Merrill AH Jr. *et al.* (2012) Modulation of ceramide synthase activity via dimerization. *J Biol Chem* 287:21025–33

Lazo ND, Meine JG, Downing DT (1995) Lipids are covalently attached to rigid corneocyte protein envelopes existing predominantly as beta-sheets: a solid-state nuclear magnetic resonance study. *J Invest Dermatol* 105:296–300

Levy M, Futerman AH (2010) Mammalian ceramide synthases. *IUBMB Life* 62:347–56

Lopez O, Cocera M, Parra JL *et al.* (1999) Influence of ceramides in the solubilization of stratum corneum lipid liposomes by C(12)-betaine/sodium dodecyl sulfate mixtures. *Int J Pharm* 187:231–41

Marekov LN, Steinert PM (1998) Ceramides are bound to structural proteins of the human foreskin epidermal cornified cell envelope. *J Biol Chem* 273:17763–70

Masukawa Y, Narita H, Shimizu E *et al.* (2008) Characterization of overall ceramide species in human stratum corneum. *J Lipid Res* 49:1466–76

Mesika A, Ben-Dor S, Laviad EL *et al.* (2007) A new functional motif in Hox domain-containing ceramide synthases: identification of a novel region flanking the Hox and TLC domains essential for activity. *J Biol Chem* 282:27366–73

Mizutani Y, Kihara A, Chiba H *et al.* (2008) 2-Hydroxy-ceramide synthesis by ceramide synthase family: enzymatic basis for the preference of FA chain length. *J Lipid Res* 49:2356–64

Mizutani Y, Kihara A, Igarashi Y (2006) LASS3 (longevity assurance homologue 3) is a mainly testis-specific (dihydro)ceramide synthase with relatively broad substrate specificity. *Biochem J* 398:531–8

Montero-Moran G, Caviglia JM, McMahon D *et al.* (2010) CGI-58/ABHD5 is a coenzyme A-dependent lysophosphatidic acid acyltransferase. *J Lipid Res* 51:709–19

Mullen TD, Hannun YA, Obeid LM (2012) Ceramide synthases at the centre of sphingolipid metabolism and biology. *Biochem J* 441:789–802

Nemes Z, Marekov LN, Fesus L *et al.* (1999) A novel function for transglutaminase 1: attachment of long-chain omega-hydroxyceramides to involucrin by ester bond formation. *Proc Natl Acad Sci USA* 96:8402–7

Ng PC, Henikoff S (2001) Predicting deleterious amino acid substitutions. *Genome Res* 11:863–74

Oji V, Tadini G, Akiyama M *et al.* (2010) Revised nomenclature and classification of inherited ichthyoses: results of the First Ichthyosis Consensus Conference in Soreze 2009. *J Am Acad Dermatol* 63:607–41

Oji V, Traupe H (2009) Ichthyosis: clinical manifestations and practical treatment options. *Am J Clin Dermatol* 10:351–64

Pewzner-Jung Y, Ben-Dor S, Futerman AH (2006) When do Lasses (longevity assurance genes) become CerS (ceramide synthases)?: Insights into the regulation of ceramide synthesis. *J Biol Chem* 281:25001–5

Rabionet M, van der Spoel AC, Chuang CC *et al.* (2008) Male germ cells require polyenoic sphingolipids with complex glycosylation for completion of meiosis: a link to ceramide synthase-3. *J Biol Chem* 283:13357–69

Radner FP, Streith IE, Schoiswohl G *et al.* (2010) Growth retardation, impaired triacylglycerol catabolism, hepatic steatosis, and lethal skin barrier defect in mice lacking comparative gene identification-58 (CGI-58). *J Biol Chem* 285:7300–11

Rheinwald JG, Green H (1974) Growth of cultured mammalian cells on secondary glucose sources. *Cell* 2:287–93

Rüschendorf F, Nürnberg P (2005) ALOHOMORA: a tool for linkage analysis using 10K SNP array data. *Bioinformatics* 21:2123–5

Schmuth M, Gruber R, Elias PM *et al.* (2007) Ichthyosis update: towards a function-driven model of pathogenesis of the disorders of cornification and the role of corneocyte proteins in these disorders. *Adv Dermatol* 23:231–56

Schwamb J, Feldhaus V, Baumann M *et al.* (2012) B-cell receptor triggers drug sensitivity of primary CLL cells by controlling glucosylation of ceramides. *Blood* 120:3978–85

Shaner RL, Allegood JC, Park H *et al.* (2009) Quantitative analysis of sphingolipids for lipidomics using triple quadrupole and quadrupole linear ion trap mass spectrometers. *J Lipid Res* 50:1692–707

Signorelli P, Hannun YA (2002) Analysis and quantitation of ceramide. *Methods Enzymol* 345:275–94

Spassieva S, Seo JG, Jiang JC *et al.* (2006) Necessary role for the Lag1p motif in (dihydro)ceramide synthase activity. *J Biol Chem* 281:33931–8

Teufel A, Maass T, Galle PR *et al.* (2009) The longevity assurance homologue of yeast lag1 (Lass) gene family. *Int J Mol Med* 23:135–40

Uchida Y, Cho Y, Moradian S *et al.* (2010) Neutral lipid storage leads to acylceramide deficiency, likely contributing to the pathogenesis of Dorfman-Chanarin syndrome. *J Invest Dermatol* 130:2497–9

Uchida Y, Holleran WM (2008) Omega-O-acylceramide, a lipid essential for mammalian survival. *J Dermatol Sci* 51:77–87

van den Ent F, Löwe J (2006) RF cloning: a restriction-free method for inserting target genes into plasmids. *J Biochem Biophys Methods* 67:67–74

van Smeden J, Hoppel L, van der Heijden R *et al.* (2011) LC/MS analysis of stratum corneum lipids: ceramide profiling and discovery. *J Lipid Res* 52:1211–21

Zheng Y, Yin H, Boeglin WE *et al.* (2011) Lipoxygenases mediate the effect of essential fatty acid in skin barrier formation: a proposed role in releasing omega-hydroxyceramide for construction of the corneocyte lipid envelope. *J Biol Chem* 286:24046–56